Spatial variability of the parameters of soil-water characteristic curves in gravel-mulched fields

Wenju Zhao, Taohong Cao, Zongli Li, Yu Su and Zhiwei Bao

ABSTRACT

Knowledge of the soil-water characteristic curve (SWCC) and its spatial variability is essential for many agricultural, environmental, and engineering applications. We analyzed the spatial variability of the parameters of SWCC in gravel-mulched fields using classical statistics and geostatistical methods. Soil samples were collected from the layer in 64 evenly distributed 1×1 m quadrats 4 m apart, center to center. SWCC in the gravel-mulched fields could be fitted well by both the van Genuchten and Brooks–Corey models, but the fit was better with the van Genuchten model. The type of fitting three parameters was tested. The model parameters θ_s and n of each type of soil were weakly variable, and α was moderately variable. The results indicate that the gravel-mulched field has better water retention, and the water retention effect of the new gravel-mulched fields is most obvious. The spatial variation of the parameters in SWCC can therefore be used to infer soil hydraulic properties, which is important for simplifying the calculation of SWCC and quantitatively determining the retention of soil water and for managing the capacity of soil to retain water in gravel-mulched fields in arid regions.

Key words | gravel-mulched fields, model parameters, soil-water characteristic curve, spatial variability

Wenju Zhao (corresponding author)
Taohong Cao
Yu Su
Zhiwei Bao
College of Energy and Power Engineering,
Lanzhou University of Technology,
Lanzhou 730050,
China
E-mail: *wenjuzhao@126.com*

Zongli Li
General Institute for Water Resources and Hydropower Planning and Design, Ministry of Water Resources,
Beijing 100120,
China

INTRODUCTION

The soil-water characteristic curve (SWCC) defines the relationship between soil suction and water-holding capacity (saturation, *Sr*, mass water content, ω, or volumetric water content, θ) (Hardie *et al.* 2013; Chen *et al.* 2015; Wang *et al.* 2017a). SWCC is indispensable input data for the simulation in agriculture, landscape management, water-resources engineering and all possible environmental incidences of assorted fields. However, the direct measurement is troublesome, time-consuming and expensive. Researchers around the world have developed many methods for determining SWCC (Ishimwe *et al.* 2014; Haghverdi *et al.* 2018) and have proposed many empirical formulas to describe the relationship between volumetric soil-water content (SWC) and soil-water suction. The van Genuchten (VG) model (van Genuchten 1980) and its modified model, the Brooks–Corey (BC) model (Brooks & Corey 1964), and the dual-porosity (Durner 1994) and log-normal-distribution (Kosugi 1996) models are commonly used. This work is focused on finding out the optimal model and analyzing the spatial variability of the parameters of soil-water characteristic curves in gravel-mulched fields.

SWCC and suitable models have been well studied. Xing *et al.* (2015b) found that the effective shrinkage of soil satisfied a logarithmic relationship with suction. Wang *et al.* (2017b) reported that the residual water content, θ_r, decreased as soil-water suction increased and that the numerical values of the fitting parameters α and n did not vary significantly. Zheng *et al.* (2014) proposed that the SWC of a plant mixed with the same soil-water suction was higher than that of pure soil. Fattah *et al.* (2017) found that suction decreased sharply as the initial water content increased and that an increase in bentonite content slightly affected SWCC. Mohammadi & Meskini-Vishkaee (2013) constructed SWCCs from data for the distribution of

doi: 10.2166/ws.2019.153

soil-particle size and bulk density using a packing-density scaling factor. Xie *et al.* (2018) suggested that the wetting SWCC can provide reasonable prediction of collapse behaviour due to wetting.

Gravel-sand mulches on soil surfaces is an indigenous technology used for crop yield for at least 300 years in the loess area of northwest China (Hao *et al.* 2017; Wang *et al.* 2018). Covering the soil surface with sand and gravel can substantially reduce surface runoff and can affect infiltration, steam reduction, heat preservation and corrosion resistance (Xi *et al.* 2016; Zhai *et al.* 2016; Zhao *et al.* 2017a, 2017b). SWCC varies spatially, but direct measurement is time-consuming and laborious, which is not conducive to an accurate and efficient analysis of a large number of samples, thus limiting the simulation of soil-water movement on a large scale (Zhao *et al.* 2008; Patil & Rajput 2009). The extent of the influence of parameters on SWCC is soil-specific (Malaya & Sreedeep 2012), so we studied the spatial variability of the VG model parameters of SWCC at different planting ages. This paper is a quantitative evaluation of the VG model for accurately determining SWCC at a sampling site, which will help to establish a model of water movement, to simplify the calculation of SWCCs and provide a scientific basis for guiding the management of soil water and improving gravel-mulched fields.

MATERIALS AND METHODS

Study area

The study was conducted in Jingtai County near the Lanzhou University of Technology experimental station in the middle of the western portion of China's Gansu province (on the east side of the Hexi corridor, at the junction of the provinces (regions) of Gansu, Ningxia, and Inner Mongolia) (Figure 1). The planting area of gravel-mulched field in the study area occupies approximately 33.3 km^2. The climate is intermediate between continental monsoon and non-monsoon regions. The temperature fluctuates from −27.3 to 36.6 °C from the winter to summer seasons, with a mean annual temperature of 8.2 °C. The mean annual precipitation is 185 mm, with a rainy season (accounting for approximately 61.4% of the annual rainfall) from July to September. The mean annual evaporation is 3,038 mm, with an annual average evaporation to precipitation ratio of 16. Solar-thermal resources are rich with an annual sunshine time of about 2,725 h and a sunshine percentage of 62%.

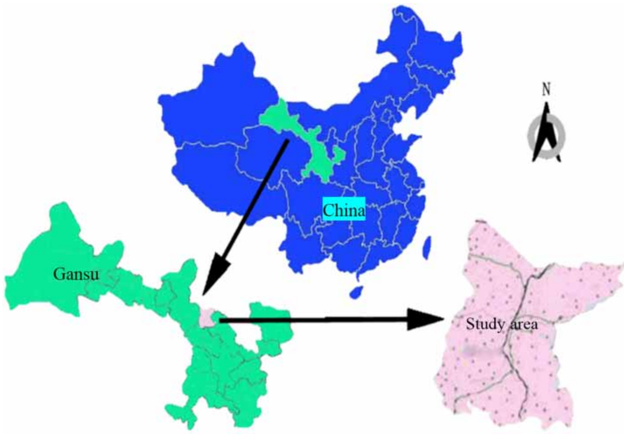

Figure 1 | Study area and the soil sampling locations in the study area situated in Gansu, China.

Test treatments

We tested three mulched fields (new gravel-mulched field (NGM) of less than 10 planting years, middle gravel-mulched field (MGM) of 25–30 years and old gravel-mulched field (OGM) of 45–60 years) and the bare land (CK) each with an area of 32×32 m. The samples were collected from the 0 to 20 cm layer in 64 evenly distributed 1×1 m quadrats 4 m apart, center to center.

Research methods

Determination of SWC: The tested soil was saturated in water before the test began. SWCs of the NGM, MGM and OGM soils were determined by weighing before and after oven-drying (at 105 °C for 8 h), which is expressed as a percentage of soil water content in dry soil weight.

Construction of SWCCs: Soil suction was measured using a Nissan CR21 high-speed constant-temperature refrigerated centrifuge. The test soils were first saturated in water and then centrifuged within a pressure range of 0–1,000 kPa. The equilibrium time increased with the applied pressure. SWC at the end of each centrifugation was obtained by weighing and converted into volumetric water content; the distance from the soil surface to the top surface of the ring cutter was measured by a vernier caliper to determine the change in bulk density during centrifugation. The relationship between the soil-matrix potential and SWC under different pressures was calculated, and SWCCs for the soils were constructed. Each treatment was repeated twice, and the means were analyzed.

Data analysis

Empirical model of the SWCCs

The VG model is:

$$\theta(h) = \begin{cases} \theta_r + \dfrac{\theta_s - \theta_r}{(1 + |\alpha h|^n)^m} & h < 0 \\ \theta_s & h \geq 0 \end{cases} \tag{1}$$

and the BC model is:

$$\frac{\theta - \theta_r}{\theta_s - \theta_r} = \begin{cases} (\alpha h)^{-n} & \alpha h > 1 \\ 1 & \alpha h \leq 1 \end{cases} \tag{2}$$

where θ is the volumetric water content (cm^3/cm^3), θ_s is the saturated volumetric water content (cm^3/cm^3), θ_r is the residual volumetric water content (cm^3/cm^3), h is the pressure head (m), α is a scaling parameter that is inversely proportional to mean pore diameter, and m and n are shape coefficients, where m and n are unrelated, $m = 1 - 1/n$ or $m = 1 - 2/n$. The value of n determines the slope of the SWCC. When n is large, the slope is large, and when n is small, the slope is small.

Geostatistical methods

A semivariogram based on the regionalized variable theory and intrinsic hypothesis (Pham 2016) is described by:

$$\gamma(h) = \frac{1}{2N(h)} \sum_{i=1}^{N(h)} [Z(x_i + h) - Z(x_i)]^2 \tag{3}$$

where h is the spatial sampling interval, $\gamma(h)$ is the semivariance for interval h, $N(h)$ is the total number of sample pairs for the separation interval h, and $Z(x_i + h)$ and $Z(x_i)$ are measured samples at points $x_i + h$ and x_i, respectively.

RESULTS AND DISCUSSION

The variation of SWCCs with the planting ages

The SWCCs for NGM, MGM and OGM had consistent morphologies (Figure 2). The SWCCs were smooth when the suction was low (<200 kPa). SWC for each treatment decreased at a faster rate as the suction increased. Soil is mainly drained through large pores, so even if the suction force varies little, SWC will vary considerably. The slope of the curve was large at intermediate and high suction (200–100 kPa), and SWC for each treatment decreased slowly as the suction increased. Only small pores can retain water at high suction, and the soil has a high water-holding capacity. SWC does not vary substantially with suction (Wang et al. 2013; Xing et al. 2016).

SWC was highest in NGM under the same suction conditions. SWC gradually decreased as planting age increased, indicating that the capacity of the soil to supply water was high in the tilled layer in NGM and that the capacity decreased with planting age. The NGM soil thus had a high water potential and low suction, so the water could be easily absorbed by the crops. The soil-water potential, however, was significantly lower in MGM, OGM and CK

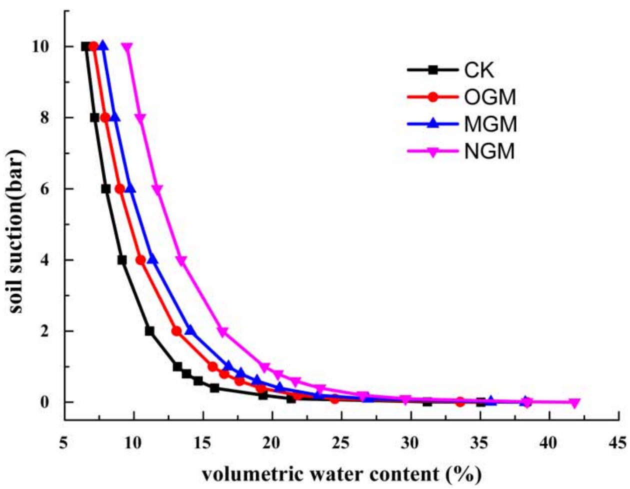

Figure 2 | The SWCCs with the planting ages.

than in NGM, and the suction was higher, which would gradually impede the use of water by the crop. Qiu et al. (2014) reported similar results in a study of the effects of gravel-sand mulching on soil physical and chemical properties.

Specific water capacity

The change in water content caused by the change in unit suction is called the specific water capacity (C). A numerical value equal to the negative slope of SWCC is an important parameter for characterizing the physical properties of the soil. At the same time, the specific water capacity curve is an important auxiliary curve for studying SWCC, which reflects the basic change nature of SWCC to some extent. It is of great significance in evaluating the effectiveness of the soil (Gao et al. 2014). Its expression is:

$$C(\theta) = Ah^B \tag{4}$$

where A is a parameter characterizing the magnitude of the specific water capacity value, and parameter B is the degree to which the water capacity changes when the soil water suction changes, and $C(\theta)$ is the specific water capacity; θ and h have the same meaning as before.

Table 1 shows the expression of tested soil specific water capacity. The greater the specific water capacity, the greater the water-holding capacity of the soil (Zhang et al. 2004). It is generally believed that the specific water volume value when the soil water suction is 100 kPa can better characterize the soil water supply capacity (Xing et al. 2015b; Shang et al. 2012). The absolute values of the specific water capacity of the four soil samples of CK, OGM, MGM and NGM at a suction force of 100 kPa are 2.86×10^{-5}, 3.28×10^{-5}, 3.51×10^{-5}, and 3.74×10^{-5} cm, that is, the NGM water supply capacity is stronger than the other three soil samples.

Table 1 | Expression of tested soil specific water capacity

Test soil	Specific water capacity expression	R^2
CK	$C(\theta) = -0.14h^{-1.23}$	0.9773
OGM	$C(\theta) = -0.1596h^{-1.229}$	0.9493
MGM	$C(\theta) = -0.1682h^{-1.227}$	0.9507
NGM	$C(\theta) = -0.1573h^{-1.208}$	0.9471

Suitable models of SWCC for the various planting ages

The VG and BC models are widely applicable, so selecting suitable Mualem (M) (Mualem 1976) and Burdine (B) (Burdine 1953) models is necessary to resolve soil unsaturated hydraulic conductivity. Six models were used to fit the SWCCs for the three planting ages based on the relationship between the parameters m and n in the VG model: VG-M (m, n), VG-M ($1 - 1/n$, n), VG-B (m, n), VG-B ($1 - 2/n$, n), BC-M and BC-B. The SWCCs for the various planting ages were fitted by the VG and BC models using RETC software (van Genuchten et al. 1991), the measured values of SWC under each suction force were compared with the fitted values and errors were analyzed (Table 2).

The calculated sum of squares (SSQ) and the coefficient of determination (R^2) were used to characterize the fitting accuracy of each model. Each model was well applicable to the tested soils of the planting ages, and R^2 tended to be >0.98. The relative errors satisfied the accuracy requirements. VG-M (m, n) was the optimal model for the soils; the SSQs of the model were the lowest, and R^2 was the highest for CK, NGM, MGM and OGM, respectively. The VG model generally simulated the SWCCs better than the BC model, and the precision was high, consistent with other results (Li et al. 2012; Xing et al. 2015b; Deng et al. 2016).

SWC was more similar to the measured SWC using the VG model. Comprehensively describing SWCCs from a mechanistic point of view remains difficult, but model suitability depends on the fitting, which is difficult to mechanistically describe (Xing et al. 2015a, 2015b).

Analysis of spatial variability of the parameters of SWCCs with planting age

The statistics of the VG-M ($1 - 1/n$, n) model parameters for CK, NGM, MGM and OGM are shown in Table 3; θ_r fitted by RETC was almost zero, probably because the soil was sandy loam and the residual water content was very low. We will therefore discuss only three parameters: θ_s, α and n.

Table 2 | Fitting value and fitting error of hydraulic parameters with each model

Test soil	Empirical model	θ_r	θ_s	α	n	m	R^2	$SSQ/10^{-3}$
CK	VG-M(m, n)	0.006	0.347	4.331	1.005	0.272	0.998	0.22
	VG-B(m, n)	0.012	0.337	4.845	2.005	0.134	0.992	0.74
	VG-M(1–1/n, n)	0	0.346	5.875	1.244		0.997	0.27
	VG-B(1–2/n, n)	0	0.339	6.586	2.234		0.993	0.64
	BC-M	0	0.330	4.979	0.244		0.990	0.99
	BC-B	0	0.330	4.979	0.244		0.990	0.99
NGM	VG-M(m, n)	0	0.409	2.089	1.005	0.252	0.995	0.6
	VG-B(m, n)	0	0.401	2.790	2.005	0.116	0.989	1.33
	VG-M(1–1/n, n)	0	0.406	2.447	1.242		0.993	0.86
	VG-B(1–2/n, n)	0	0.401	2.834	2.230		0.989	1.39
	BC-M	0	0.399	2.907	0.228		0.987	1.55
	BC-B	0	0.399	2.907	0.228		0.987	1.55
MGM	VG-M(m, n)	0	0.379	2.144	1.005	0.272	0.996	0.41
	VG-B(m, n)	0	0.372	2.914	2.005	0.125	0.992	0.88
	VG-M(1–1/n, n)	0	0.376	2.567	1.260		0.995	0.57
	VG-B(1–2/n, n)	0	0.371	2.955	2.248		0.992	0.93
	BC-M	0	0.370	3.003	0.246		0.991	1.04
	BC-B	0	0.370	3.003	0.246		0.991	1.04
OGM	VG-M(m, n)	0	0.374	3.239	1.005	0.261	0.993	0.79
	VG-B(m, n)	0	0.364	4.094	2.005	0.121	0.985	1.65
	VG-M(1–1/n, n)	0	0.371	3.977	1.247		0.990	1.07
	VG-B(1–2/n, n)	0	0.363	4.087	2.241		0.984	1.73
	BC-M	0	0.359	3.740	0.244		0.982	2
	BC-B	0	0.359	3.740	0.244		0.982	2

Notes: (1) θ_r and θ_s are soil residual volume water content and saturated volume water content, respectively, cm^3/cm^3; (2) if the θ_r fitting value is <0.001, the software automatically takes the value as 0.

Table 3 | Statistical results of VG-M $(1-1/n, n)$ model parameters

Model parameter	Test soil	Maximum	Minimum	Mean	Standard deviation	CV	Kurtosis	Skewness
θ_s	CK	0.381	0.363	0.374	0.004	0.010	0.938	−0.506
	NGM	0.459	0.420	0.443	0.007	0.016	0.841	0.081
	MGM	0.449	0.388	0.432	0.014	0.033	−0.112	0.663
	OGM	0.438	0.417	0.426	0.005	0.012	−0.583	0.167
α	CK	0.094	0.032	0.059	0.014	0.235	−0.152	0.344
	NGM	0.021	0.010	0.015	0.002	0.157	−0.067	0.006
	MGM	0.215	0.021	0.054	0.034	0.624	7.818	2.457
	OGM	0.034	0.012	0.021	0.004	0.211	0.153	0.431
n	CK	1.228	1.175	1.199	0.009	0.007	1.403	0.406
	NGM	1.227	1.183	1.212	0.008	0.007	2.349	−1.228
	MGM	1.269	1.176	1.225	0.019	0.016	−0.189	−0.238
	OGM	1.279	1.223	1.253	0.011	0.009	−0.066	0.054

The minimum, maximum and mean values of the VG-M $(1-1/n, n)$ model parameters for the various planting ages indicated that θ_s was larger for the gravel-mulched fields than CK, with mean θ_s in the order CK < OGM < MGM < NGM, indicating that the amount of soil mixed into the sand layer increased, and the degree of sand mixing increased, with planting age, which would affect the structure of the gravel layer and the degradation of gravel-mulched fields. The coefficient of variation (CV) indicates the variation or dispersion of a sample. CVs < 0.1 indicate low variability, $0.1 \leq$ CVs ≤ 1 indicate moderate variability and CVs > 1 indicate high variability. The CVs of θ_s and n for all soils were <0.1, indicating low variation, and the CVs of α for all soils were between 0.1 and 1, indicating moderate variation. These results were similar to those of Liu *et al.* (2010).

The skewness of the VG-M ($1 - 1/n$, n) model parameters of the soils was <1 and varied near 0, except for α in MGM and n in NGM, indicating that the parameters were normally distributed. A representative SWCC can be constructed using means, which can simplify the complicated construction of SWCCs in practical applications.

The parameters α, n and θ_s of the VG-M ($1 - 1/n$, n) model were analyzed using GS + 9.0 software (version 9.0, Gamma Design Software, Michigan, USA) to determine the spatial variability of SWC for the planting ages. The semi-variance function of the VG-M ($1 - 1/n$, n) model parameters in NGM was then graphed.

The curve of the semi-variance function of the VG-M ($1 - 1/n$, n) model parameters for NGM was relatively uniform (Figure 3), indicating that the correlation coefficient of the fitting of SWCCs was relatively high throughout the study area. The spatial correlation of the model parameters will be affected by soil organic-matter content, topography, vegetation and human activities as gravel-mulched fields age. The parameters of the SWCC model were also spatially random, which was similar to the results reported by Zhang *et al.* (2014). SWCCs therefore had different spatial correlations for the different planting ages.

Three-dimensional spatial distribution of the VG-M ($1 - 1/n$, n) model parameters

A three-dimensional spatial-distribution map of the VG-M ($1 - 1/n$, n) model parameters was prepared using Kriging interpolation to more intuitively demonstrate the spatial distribution of the SWCC VG-M ($1 - 1/n$, n) model parameters for the planting ages based on the semi-variance function model. We will use CK and NGM as examples.

The soil VG-M ($1 - 1/n$, n) model parameters differed in both the vertical and horizontal directions due to the existence of spatial variability. The Kriging maps of model parameters for each soil indicated 'bumpy and uneven' distributions (Figure 4), which may be associated

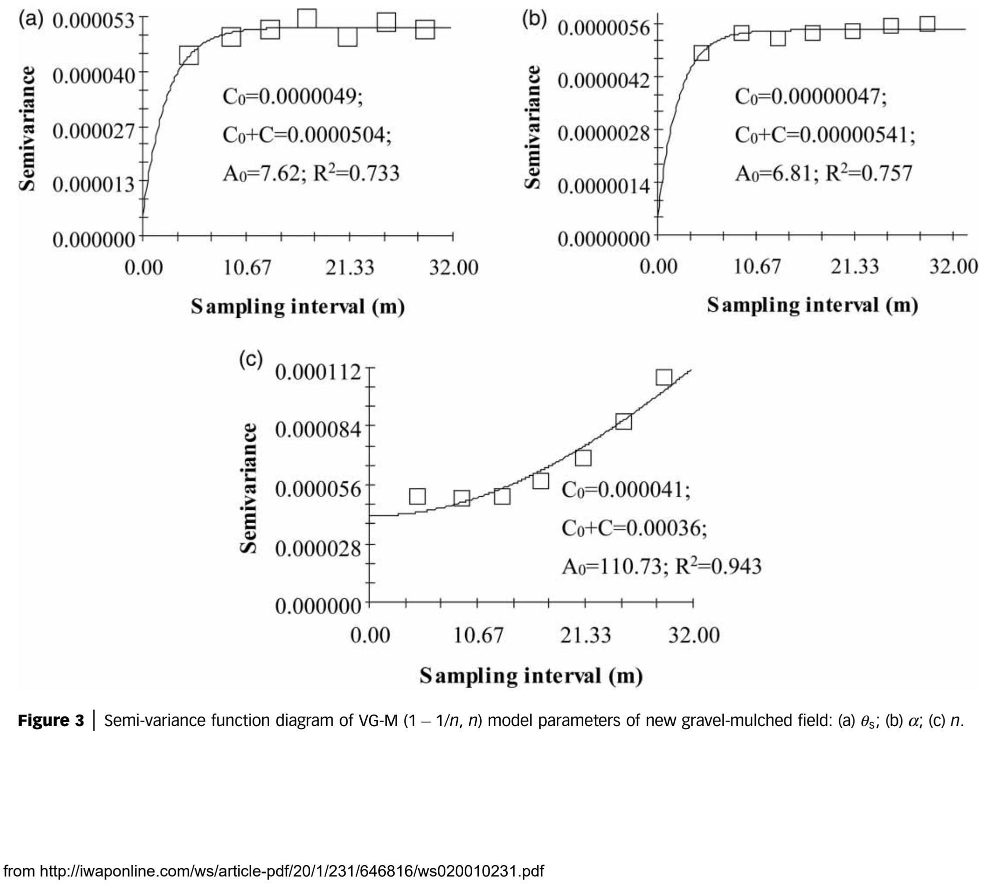

Figure 3 | Semi-variance function diagram of VG-M ($1 - 1/n$, n) model parameters of new gravel-mulched field: (a) θ_s; (b) α; (c) n.

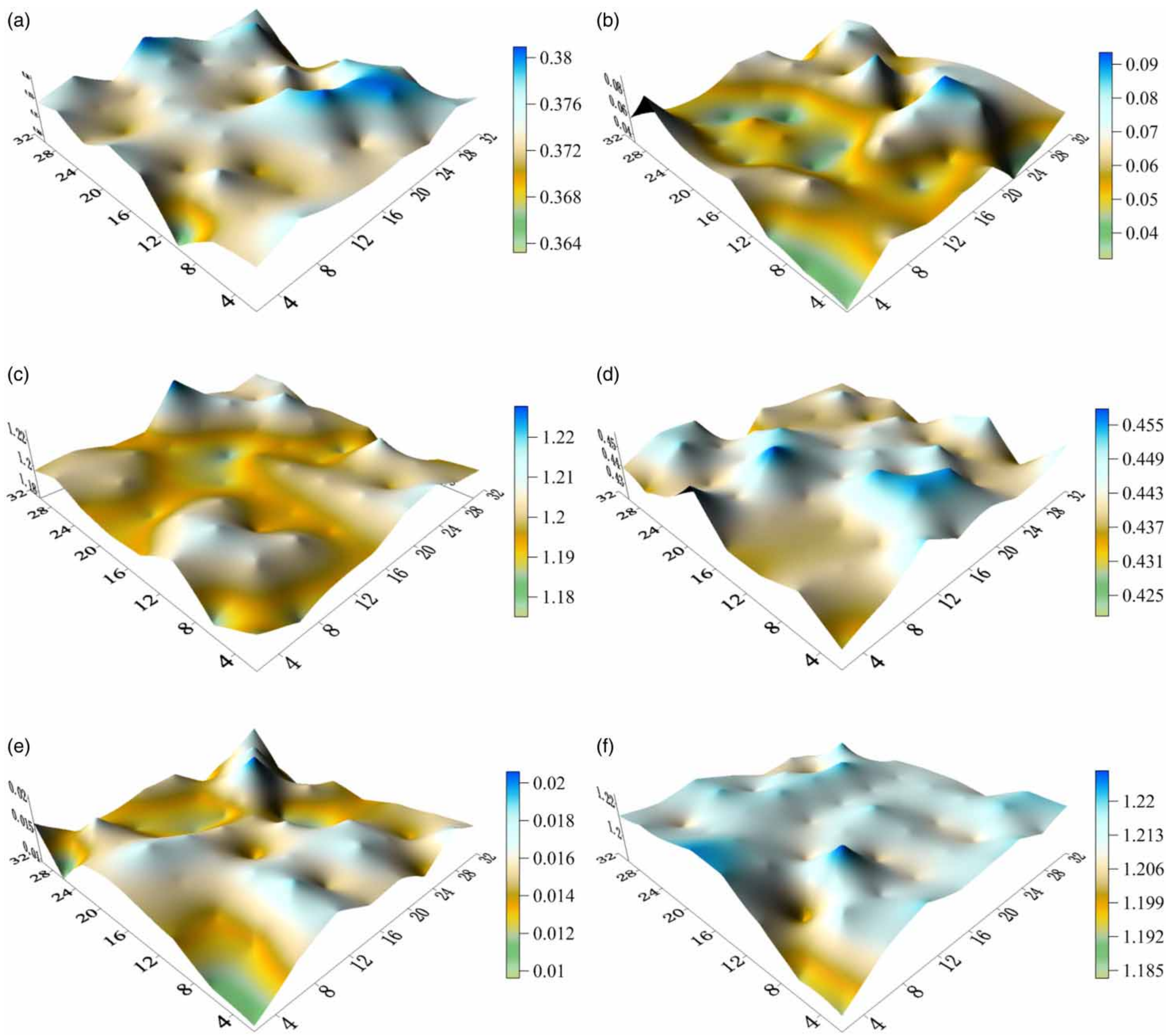

Figure 4 | Spatial distribution map of VG-M ($1-1/n$, n) model parameters of tested soil: (a) θ_s of CK; (b) α of CK; (c) n of CK; (d) θ_s of NGM; (e) α of NGM; (f) n of NGM.

with the topography in the sampling area. NGM's graphs were relatively 'flat', indicating that the VG-M ($1-1/n$, n) model parameters for NGM were strongly spatially autocorrelated, and the spatial heterogeneity caused by the spatial autocorrelation was larger than the space caused by random factors. The VG-M ($1-1/n$, n) model parameters for CK had an obvious 'bump' trend, which further indicated that the gravel-mulched field retained water well and that the water-retention effect was the most obvious in MGM.

CONCLUSIONS

The SWCCs illustrated that SWC was more variable in NGM than in MGM and OGM, indicating that soil-water conductivity was highest in NGM. Both the VG and BC models fit the SWCCs well, but the VG model was best. Each soil θ_s and n were weakly variable, α was moderately variable and the SWCCs of the gravel-mulched fields were strongly spatially autocorrelated. The VG-M ($1-1/n$, n) model parameters of three-dimensional spatial distribution for all soils had 'bumpy and uneven' distributions. The 'bump' was lowest for NGM, and the VG-M ($1 - 1/n$, n) model parameters for CK had a distinct 'bump' trend.

Evaluating the spatial variability of the parameters of SWCC in gravel-mulched fields would be beneficial to validate the utility of soil moisture data to estimate the parameters in the VG model and the spatial variability of saturated hydraulic conductivity. These results can provide valuable support for water resources management.

ACKNOWLEDGEMENTS

The research was supported by National Natural Science Foundation of China (51869010), Guidance Program for Industrial Support of Colleges and Universities in Gansu Province (2019C-13), Longyuan Youth Innovation and Entrepreneurship Project and the Lanzhou University of Technology Hongliu first-class discipline funding.

REFERENCES

Brooks, R. H. & Corey, A. T. 1964 *Hydraulic Properties of Porous Media*. Hydrology Papers 3, Colorado State University, Fort Collins, CO, USA.

Burdine, N. T. 1953 Relative permeability calculations from pore size distribution data. *Petr. Trans. Am. Inst. Mining Metall. Eng.* **198** (3), 71–78.

Chen, R., Liu, J., Li, J. H. & Ng, C. W. W. 2015 An integrated high-capacity tensiometer for measuring water retention curves continuously. *Soil Sci. Soc. Am. J.* **79** (3), 943–947.

Deng, Y., Ding, S., Cai, C. & Lü, G. 2016 Characteristic curves and model analysis of soil moisture in collapse mound profiles in Southeast Hubei. *Acta Pedol. Sin.* **53** (2), 355–364.

Durner, W. 1994 Hydraulic conductivity estimation for soils with heterogeneous pore structure. *Water Resour. Res.* **30** (2), 211–223.

Fattah, M. Y., Salim, N. M. & Irshayyid, E. J. 2017 Determination of the soil–water characteristic curve of unsaturated bentonite–sand mixtures. *Environ. Earth Sci.* **76** (5), 201.

Gao, H. Y., Guo, S. L., Liu, W. Z., Li, M. & Zhang, J. 2014 Spatial variability of soil water retention curve under fertilization practices in arid-highland of the Loess Plateau. *Trans. Chin. Soc. Agric. Mach.* **45** (6), 161–165 + 176.

Haghverdi, A., Öztürk, H. S. & Durner, W. 2018 Measurement and estimation of the soil water retention curve using the evaporation method and the pseudo continuous pedotransfer function. *J. Hydrol.* **563**, 251–259.

Hao, H. T., Zhao, X., Wang, Y., Zhang, Y. B., Xie, Z. K., Guo, Z. H. & Wang, R. Y. 2017 Effects of gravel-sand mulching on soil bacterial community and metabolic capability in the semi-arid Loess Plateau, China. *World J. Microbiol. Biotechnol.* **33** (11), 209.

Hardie, M. A., Lisson, S., Doyle, R. B. & Cotching, W. E. 2013 Evaluation of rapid approaches for determining the soil water retention function and saturated hydraulic conductivity in a hydrologically complex soil. *Soil Tillage Res.* **130**, 99–108.

Ishimwe, E., Blanchard, J. & Coffman, R. A. 2014 Field-obtained soil water characteristic curves and hydraulic conductivity functions. *J. Irrig. Drain. Eng.* **144** (1), 04017056.

Kosugi, K. 1996 Lognormal distribution model for unsaturated soil hydraulic properties. *Water Resour. Res.* **32** (9), 2697–2703.

Li, X., Zhou, J., Jin, M. & Liu, Y. 2012 Soil-water characteristic curves of high-TDS and suitability of fitting models. *Trans. Chin. Soc. Agric. Eng.* **28** (13), 135–141.

Liu, J. L., Ma, X. Y. & Zhang, Z. H. 2010 Spatial variability of soil water retention curve in different soil layers and its affecting factors. *Trans. Chin. Soc. Agric. Mach.* **41** (1), 46–52.

Malaya, C. & Sreedeep, S. 2012 Critical review on the parameters influencing soil-water characteristic curve. *J. Irrig. Drain. Eng.* **138** (1), 55–62.

Mohammadi, M. H. & Meskini-Vishkaee, F. 2013 Predicting soil moisture characteristic curves from continuous particle-size distribution data. *Pedosphere* **23** (1), 70–80.

Mualem, Y. 1976 A new model for predicting the hydraulic conductivity of unsaturated porous media. *Water Resour. Res.* **12** (3), 513–522.

Patil, N. G. & Rajput, G. S. 2009 Evaluation of water retention functions and computer program 'Rosetta' in predicting soil water characteristics of seasonally impounded shrink–swell soils. *J. Irrig. Drain. Eng.* **135** (3), 286–294.

Pham, T. D. 2016 The semi-variogram and spectral distortion measures for image texture retrieval. *IEEE Trans. Image Process* **25** (4), 1556–1565.

Qiu, Y., Wang, Y. & Xie, Z. 2014 Long-term gravel–sand mulch affects soil physicochemical properties, microbial biomass and enzyme activities in the semi-arid Loess Plateau of North-western China. *Acta Agric. Scand., Sec. B – Soil Plant Sci.* **64** (4), 294–303.

Shang, M. T., Zhang, J. Y., Liu, J. F. & Wang, X. J. 2012 Effects of macropore on soil specific water capacity and unsaturated hydraulic conductivity. *J. Irrig. Drain.* **31** (2), 1–5.

van Genuchten, M. T. 1980 A closed-form equation for predicting the hydraulic conductivity of unsaturated soils. *Soil Sci. Soc. Am. J.* **44** (5), 892–898.

van Genuchten, M. T., Leij, F. J. & Yates, S. R. 1991 *The RETC Code for Quantifying the Hydraulic Functions of Unsaturated Soils: Project Summary*. EPA/600/2-91/065, Robert S. Kerr Environmental Research Laboratory, USEPA, Ada, OK, USA.

Wang, Z. J., Jiang, Q., He, J. L. & Kun, M. A. 2013 Analysis of soil water characteristic curve and infiltration rates of gravel-mulched land around Xiangshan Mountain area in Ningxia. *Chin. J. Soil Sci.* **44** (6), 1364–1368.

Wang, S., Cheng, M., Li, X., Wang, X., Mao, X. & Yang, H. 2017a Establishment of generalized soil-water characteristic curve theoretical model considering two stress state variables for unsaturated soils. *Trans. Chin. Soc. Agric. Eng.* **33** (6), 1–7.

Wang, T., Ding, Y. M., Zhao, X. W., Liu, B. G. & Song, Y. 2017b Experimental study on the soil-water characteristic curve of the unsaturated loess in East Gansu province. *Bulg. Chem. Commu.* **49**, 165–171.

Wang, D. L., Feng, H., Liu, X. Q., Li, Y., Zhou, L. F., Zhang, A. F. & Dyck, M. 2018 Effects of gravel mulching on yield and multilevel water use efficiency of wheat-maize cropping system in semi-arid region of Northwest China. *Field Crop Res.* **218**, 201–212.

Xi, H. Y., Feng, Q., Zhang, L., Si, J. H., Chang, Z. Q., Yu, T. F. & Guo, R. 2016 Effects of water and salinity on plant species composition and community succession in Ejina Desert Oasis, northwest China. *Environ. Earth Sci.* **75** (2), 138.

Xie, W. L., Li, P., Vanapalli, S. K. & Wang, J. D. 2018 Prediction of the wetting-induced collapse behaviour using the soil-water characteristic curve. *J. Asian Earth Sci.* **151**, 259–268.

Xing, X., Zhao, W., Liu, Y. & Ma, X. 2015a Spatial variability of soil moisture in kiwi field under different sampling density conditions. *Trans. Chin. Soc. Agric. Mach.* **46** (8), 138–145.

Xing, X., Zhao, W., Ma, X. & Zhang, Y. 2015b Study on soil shrinkage characteristics during soil water characteristic curve measurement. *J. Hydraul. Eng.* **46** (10), 1181–1188.

Xing, X., Liu, Y. & Ma, X. 2016 Effects of soil additive on soil-water characteristic curve and soil shrinkage. *Adv. Water Sci.* **27** (1), 40–48.

Zhai, Q., Rahardjo, H. & Satyanaga, A. 2016 Variability in unsaturated hydraulic properties of residual soil in Singapore. *Eng. Geol.* **209**, 21–29.

Zhang, Q., Sun, X. Y., Yu, W. P. & Huang, L. J. 2004 Studies on soil water characteristic curves and infiltration capability of Maowusu sandy soil. *For. Res.* **17**, 9–14.

Zhang, N., Qu, Z., Yang, X. & Fu, X. 2014 Application and adaptability evaluation of Bayesian model in soil transfer functions. *Trans. Chin. Soc. Agric. Mach.* **45** (2), 149–155.

Zhao, A., Huang, M. & Shi, Z. 2008 Evaluation of two indirect methods to estimate soil water characteristic curve of loess soil. *Trans. Chin. Soc. Agric. Eng.* **24** (9), 11–15.

Zhao, W. J., Cui, Z., Zhang, J. Y. & Jin, J. 2017a Temporal stability and variability of soil-water content in a gravel-mulched field in northwestern China. *J. Hydrol.* **552**, 249–257.

Zhao, W. J., Sheng, J., Li, Z. L., Ma, H. & Yu, P. 2017b Spatial variability of soil salinity in a gravel-sand mulched jujube orchard at different scales. *J. Irrig. Drain. Eng.* **143** (6), 04017009.

Zheng, J., Wang, Y., Cai, H. J., Wan, J. X. & Li, Z. J. 2014 Soil-water characteristic curves of soil with plant additive and analyses of the fitting models. *Trans. Chin. Soc. Agric. Mach.* **45** (5), 107–112.

First received 1 July 2019; accepted in revised form 12 October 2019. Available online 29 October 2019